



Supporting Information

© Wiley-VCH 2008

69451 Weinheim, Germany

A Caged Retinoic Acid for Use with One- and Two-Photon Excitation in Zebrafish Embryos

Pierre Neveu,^{[a],[b]} Isabelle Aujard,^[b] Chouaha Benbrahim,^[b] Thomas Le Saux,^[b]
Jean-François Allemand,^[a] Sophie Vríz,^{[c],[d]} David Bensimon,^[a] Ludovic Jullien^{[b],*}

[a] *Dr. P. Neveu, Dr. J. F. Allemand, Dr. D. Bensimon,*
Ecole Normale Supérieure,

Laboratoire de Physique Statistique and Département de Biologie
UMR 8550, 24 rue Lhomond, F-75231 Paris, France

[b] *Dr. P. Neveu, Dr. I. Aujard, C. Benbrahim, Dr. T. Le Saux, Prof. Dr. L. Jullien,*
Ecole Normale Supérieure,
Département de Chimie,

UMR CNRS-ENS-UPMC Paris 06 8640 PASTEUR,
24 rue Lhomond, F-75231 Paris, France

[c] *Prof. Dr. S. Vríz,*
Inserm U770, Hémostase et Dynamique Cellulaire Vasculaire,
80 rue du Général Leclerc, 94276 Le Kremlin-Bicêtre, France

[d] *Prof. Dr. S. Vríz,*
Université Paris 7 Denis Diderot, 75005 Paris, France

Supporting Information

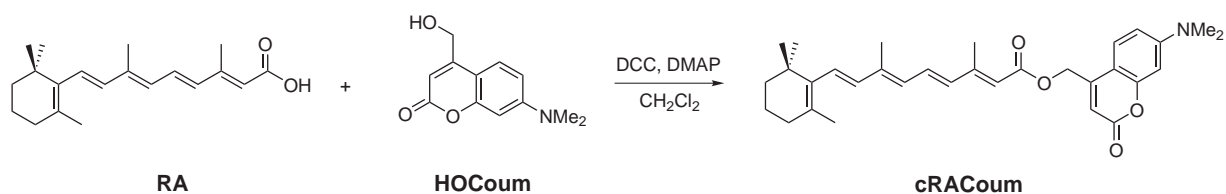
The Supporting Information reports on:

- The Experimental Methods.
- The one-photon photoconversion kinetics of **cRA** upon UV illumination.
- The comparison of the phenotypes from **RA** and two cis-retinoic acids.
- The teratogenic effects induced by UV illumination of **cRA** in injected embryos.
- The two-photon uncaging kinetics of **cRA** *in vivo*.

Experimental Methods

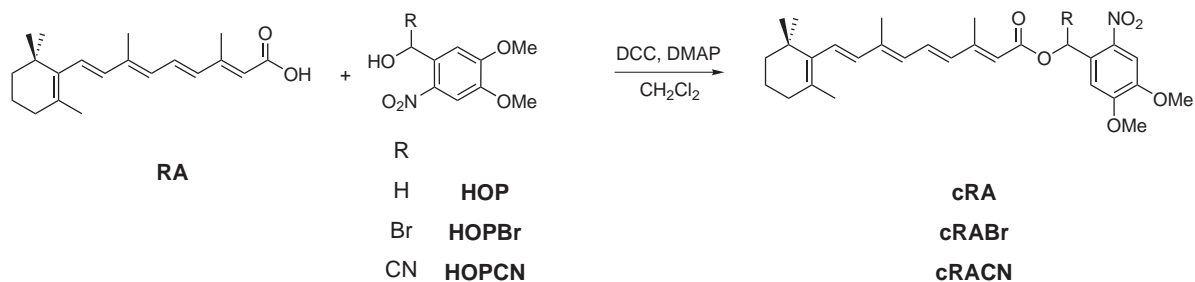
Syntheses of the caged compounds obtained from all-*trans* retinoic acid RA

The 7-dimethylamino-coumarin-4-ylmethyl ester **cRACoum** was prepared by condensation between **RA** and the 7-dimethylamino-coumarin-4-yl methanol **HOCoum** [1] in the presence of DCC (scheme 1Sa).



Scheme 1Sa. Synthesis of **cRACoum**.

The three 2-nitrobenzyl esters: **cRA**, **cRABr**, and **cRACN** were obtained under similar conditions by condensation between **RA** and the corresponding 2-nitrobenzyl alcohols **HOP**, **HOPBr**, and **HOPCN** [2] (Scheme 1Sb).



Scheme 1Sb. Syntheses of the 2-nitrobenzyl esters of **cRA**, **cRABr**, and **cRACN**.

General

The commercially available chemicals were used without further purification. Anhydrous solvents were freshly distilled before use. Column chromatography (CC): silica gel 60 (0.040-0.063 mm) Merck. Analytical and thin layer chromatography (TLC): Merck silica gel 60 F₂₅₄ precoated plates; detection by UV (254 nm). Melting point: Büchi 510. ¹H-NMR Spectra: AM-250 or 400 AVANCE Bruker; chemical shifts (δ) in ppm related to protonated solvent as internal reference (¹H: CHCl₃ in CDCl₃, 7.26 ppm; CHD₂SOCD₃ in CD₃SOCD₃, 2.49 ppm. ¹³C: ¹³CDCl₃ in CDCl₃, 77.0 ppm; ¹³CD₃SOCD₃ in CD₃SOCD₃, 39.6 ppm); Coupling constants J in Hz. Mass spectrometry (chemical ionization and high resolution with NH₃ or CH₄) was performed at the Service de Spectrométrie de masse

de l'ENS. Microanalyses were obtained from the Service de Microanalyses de l'Université Pierre et Marie Curie, Paris.

Experimental Procedures

3,7-Dimethyl-9-(2,6,6-trimethyl-cyclohex-1-enyl)-nona-2,4,6-trienoic acid 7-dimethylamino-2-oxo-2-*H*-chromen-4-ylmethyl ester (cRACoum). Same as for **cRA**. 1,3-Dicyclohexylcarbodiimide (68 mg, 0.33 mmol, 1 eq), all-*trans* retinoic acid (98 mg, 0.33 mmol), 7-dimethylamino-2-oxo-2-*H*-chromen-4-ylmethanol **HOCoum** (90 mg, 0.41 mmol, 1.25 eq; [1]), 4-dimethylaminopyridine (34 mg, 0.33 mmol, 1 eq). After purification by column chromatography on silica gel with methylene chloride as eluent, **cRACoum** as a yellow powder (132 mg, 84%). ¹H NMR (ppm, 250 MHz, CDCl₃) δ= 7.35 (d, 1 H, J=8.9 Hz), 7.06 (dd, 1 H, J= 11.5 Hz and J= 15 Hz), 6.62 (dd, 1 H, J= 2.2 Hz and J=8.9 Hz), 6.53 (d, 1 H, J=2.2 Hz), 6.31 (d, 2 H, J= 15.5 Hz), 6.16 (d, 1 H, J= 10.6 Hz), 6.15 (d, 1 H, J= 17,0 Hz), 5.87 (s, 1 H), 5.27 (s, 2 H), 3.05 (s, 6 H), 2.39 (s, 3 H), 2.04-2.01 (m, 5 H), 1.72 (s, 3 H), 1.64-1.57 (m, 2 H), 1.48-1.44 (m, 2 H), 1.03 (s, 6 H); MS (CI, CH₄): m/z 502 (calcd av mass for C₃₂H₄₀NO₄: 502.29); MS (CI, CH₄, HR): m/z 502.2952 (calcd av mass for C₃₂H₄₀NO₄: 502.2957).

3,7-Dimethyl-9-(2,6,6-trimethyl-cyclohex-1-enyl)-nona-2,4,6-trienoic acid 4,5-dimethoxy-2-nitrobenzyl ester (cRA). 1,3-Dicyclohexylcarbodiimide (103 mg, 0.5 mmol, 1 eq) was added to a solution of all-*trans* retinoic acid (150 mg, 0.5 mmol), 4,5-dimethoxy-2-nitrobenzyl alcohol **HOP** (106 mg, 0.5 mmol, 1 eq) and 4-(dimethylamino)-pyridine (61 mg, 0.5 mmol, 1 eq) in dry dichloromethane (5 mL) at 0°C under nitrogen. After 10 min at 0°C, the mixture was stirred at room temperature in the absence of light for 12 h. After filtration, the filtrate was washed with 1.2 M hydrochloric acid and saturated aqueous sodium hydrogen carbonate, then dried over sodium sulfate, and concentrated under vacuum. **cRA** was obtained as a yellow powder after precipitation in methanol (150 mg, 60%). m.p. 113°C; ¹H NMR (ppm, 400 MHz, CDCl₃, 25°C) δ= 7.72 (s, 1 H), 7.04 (dd, 1 H, J=11.0 Hz and 15.0 Hz), 7.02 (s, 1 H), 6.31 (d, 1 H, J=15.0 Hz), 6.29 (d, 1 H, J=16.1 Hz), 6.15 (d, 1 H, J=11.0 Hz), 6.14 (d, 1 H, J=16.1 Hz), 5.88 (s, 1 H), 5.56 (s, 2 H), 3.96 (s, 3 H), 3.95 (s, 3 H), 2.37 (d, 3 H, J=0.81 Hz), 2.01 (m, 2 H), 2.00 (s, 3 H), 1.71 (s, 3 H), 1.60 (m, 2 H), 1.46 (m, 2 H), 1.02 (s, 6 H); ¹³C NMR (ppm, 100 MHz, CDCl₃, 25°C) δ= 166.3, 154.4, 153.4, 148.0, 140.2, 137.6, 137.1, 134.7, 131.7, 130.1, 129.2, 129.0, 127.9, 117.1, 110.1, 108.1, 62.4, 56.3, 56.3, 39.5, 34.2, 33.0, 28.9, 21.7, 19.1, 13.9, 12.9; elemental analysis calcd (%) for C₂₉H₃₇NO₆(495.61): C 70.28, H 7.52, N 2.83; found : C 70.09, H 7.73, N 2.63; MS (CI, CH₄) : m/z 496.27 (calcd av mass for

C₂₉H₃₇NO₆ : 495.61); MS (CI, CH₄, HR) : m/z 496.2693 (calcd av mass for C₂₉H₃₈NO₆ : 496.2699).

3,7-Dimethyl-9-(2,6,6-trimethyl-cyclohex-1-enyl)-nona-2,4,6-trienoic acid 2,2,2-tribromo-1-(4,5-dimethoxy-2-nitro-phenyl)-ethyl ester (cRABr). Same as for **cRA**. 1,3-Dicyclohexylcarbodiimide (52 mg, 0.25 mmol, 1 eq), all-*trans* retinoic acid (75 mg, 0.25 mmol), 2,2,2-tribromo-1-(4,5-dimethoxy-2-nitrophenyl)ethanol **HOPBr** [2] (145 mg, 0.31 mmol, 1.25 eq), 4-dimethylaminopyridine (30 mg, 0.25 mmol, 1 eq). After purification by column chromatography on silica gel with cyclohexane/ethyl acetate: 9/1 as eluent, **cRABr** as a yellow oil (165 mg, 88%). ¹H NMR (ppm, 250 MHz, CDCl₃, 25°C) δ= 7.79 (s, 1 H), 7.57 (s, 1 H), 7.41 (s, 1 H), 7.01 (dd, 1 H, J=15.0 Hz, J=11.4 Hz), 6.31 (d, 1 H, J=15.0 Hz), 6.25 (d, 1 H, J=15.6 Hz), 6.09 (d, 1 H, J=13.6 Hz), 6.08 (d, 1 H, J=15.6 Hz), 5.90 (s, 1 H), 3.92 (s, 3 H), 3.90 (s, 3 H), 2.32 (s, 3 H), 1.94 (s, 3 H), 1.85 (m, 2 H), 1.64 (s, 3 H), 1.54 (m, 2 H), 1.38 (m, 2 H), 0.95 (s, 6 H); ¹³C NMR (ppm, 100 MHz, CDCl₃, 25°C) δ= 163.9, 163.1, 156.9, 155.1, 152.1, 149.3, 142.9, 140.9, 137.6, 137.2, 134.3, 132.6, 130.3, 129.4, 129.1, 123.4, 115.6, 111.4, 108.2, 73.3, 56.5, 56.4, 39.5, 33.1, 28.9, 21.7, 19.1, 14.2, 12.9; MS (CI, NH₃): m/z 763.0, 745.9 (calcd av mass for C₃₀H₄₀N₂O₆Br₃: 763.0, calcd av mass for C₃₀H₃₆NO₆Br₃ : 746.32); MS (CI, NH₃, HR): m/z 763.0406 and 765.0383 (calcd av mass for C₃₀H₄₀N₂O₆Br₃: 763.0418 and 765.0401).

3,7-Dimethyl-9-(2,6,6-trimethyl-cyclohex-1-enyl)-nona-2,4,6-trienoic acid cyano-(4,5-dimethoxy-2-nitro-phenyl)-methyl ester (cRACN). Same as for **cRA**. 1,3-Dicyclohexylcarbodiimide (103 mg, 0.5 mmol, 1 eq), all-*trans* retinoic acid (150 mg, 0.5 mmol), hydroxy-(4,5-dimethoxy-2-nitrophenyl)acetonitrile **HOPCN** [2] (150 mg, 0.62 mmol, 1.25 eq), 4-dimethylaminopyridine (61 mg, 0.5 mmol, 1 eq). **cRACN** as a yellow powder (270 mg, 48%). m.p. 145°C; ¹H NMR (ppm, 400 MHz, CDCl₃, 25°C) δ= 7.74 (s, 1 H), 7.18 (s, 1 H), 7.10 (dd, 1 H, J=12.3 Hz and 15.1 Hz), 6.33 (d, 1 H, J=15.1 Hz), 6.30 (d, 1 H, J=14.6 Hz), 6.15 (d, 1 H, J=12.3 Hz), 6.14 (d, 1 H, J=14.6 Hz), 6.17 (s, 1 H), 5.82 (s, 1 H), 4.03 (s, 3 H), 3.98 (s, 3 H), 2.38 (s, 3 H), 2.02 (s, 3 H), 2.02 (m, 2 H), 1.71 (s, 3 H), 1.61 (m, 2 H), 1.46 (m, 2 H), 1.02 (s, 6 H); ¹³C NMR (ppm, 100 MHz, CDCl₃, 25°C) δ= 163.9, 157.7, 153.8, 149.7, 141.3, 139.8, 137.6, 137.0, 134.0, 133.1, 130.4, 129.6, 129.1, 122.3, 115.8, 114.4, 110.0, 108.4, 58.8, 56.7, 56.5, 39.5, 34.2, 33.1, 28.9, 21.7, 19.1, 14.2, 12.9; MS (CI, NH₃): m/z 521 (calcd av mass for C₃₀H₃₆N₂O₆ : 520.62); MS (CI, NH₃, HR): m/z 521.2657 (calcd av mass for C₃₀H₃₇N₂O₆: 521.2652).

Experiments with one-photon excitation

UV illumination

All one-photon excitation experiments were performed at 20°C by putting a bench top UV lamp (365 nm;¹ 6 W; Fisher Bioblock) above a glass Petri dish (diameter: 5.5 cm) containing $V = 20$ mL of solution. We used the uncaging experiment performed with the model caged compound **PheP** to derive an order of magnitude of the photon flux \mathcal{I}_0 of the incident beam in the wavelength range leading to uncaging. By taking $\mathcal{Q}_u^{(1)} = \varepsilon_u^{(1)}\Phi_u^{(1)} = 48 \text{ M}^{-1}\text{cm}^{-1}$, [2] $V = 20$ mL, and $l = 0.9$ cm, $\mathcal{I}_0 \approx 4 \cdot 10^{-5} \text{ Einstein min}^{-1}$ was obtained from k_2 . [2]

We checked that, when illuminated for up to 4 minutes under the present conditions, control embryos developed normally (data not shown). [3] We also verified that the side product resulting from uncaging was not responsible of the observed phenotypes (data not shown).

Capillary electrophoresis

Electrophoretic measurements were performed with a PACE/MDQ (Beckman Coulter) capillary electrophoresis system. Migrations were performed at 20 kV in bare fused silica capillaries (Polymicro, Phoenix, AZ), 50 μm I.D. \times 50 cm filled with running buffer (15 mM $\text{Na}_2\text{B}_4\text{O}_7$ and 20 mM αCD containing 10% (v/v) acetonitrile; [4]) at 25°C. The analytes were detected by UV absorbance at 350 nm. In view of the similarity of the absorption spectra of the three analyzed retinoic acids at that wavelength, we assimilated the corrected areas of the peaks to the amounts of the corresponding retinoic acids.

Preliminary screening of the caged retinoic acids

Zebrafish embryos were maintained at 28°C. [5] The compounds were assayed by injecting zebrafish embryos (number of embryos injected: 50-100 range) at the 32-cell stage with 5 nl of 0.1 mM of the investigated substrate. Embryos were illuminated for various durations with the 365 nm UV lamp placed on top of the dish. They were checked for developmental abnormalities beyond 30 hours post fertilization (hpf) and compared with those incubated with (or without) known concentrations of **RA**.

Teratogenicity assay

Zebrafish embryos were maintained at 28°C. The teratogenicity of the various compounds was assayed by incubating pronase dechorionated zebrafish embryos (number of embryos

¹The lamp spectrum provided by the lamp purchaser is essentially gaussian around 350 nm with a 40 nm width at half height.

treated: 50-100 range) at the 128-cell stage for 90 min in embryo medium² [5] supplemented with 10 μM of the investigated substrate. After washing with plain embryo medium, the embryos were put in the Petri dish introduced above and illuminated for various durations with the 365 nm UV lamp placed on top of the dish. They were checked for developmental abnormalities beyond 30 hpf and compared with those incubated with (or without) known concentrations of **RA**.

***In vivo* RA degradation**

Embryos were injected at 32 cell stage with 5 nl of 0.1 mM **cRA** (final intra-cellular concentration 10 μM , number of embryos injected: 50-100 range). Embryos were put in the Petri dish introduced above and illuminated for various duration with the 365 nm UV lamp placed on top of the dish. They were checked for developmental abnormalities beyond 30 hpf.

Experiments with two-photon excitation

Instrumental setup

For the *in vivo* uncaging calibration studies, a home-built microscope [6] equipped with an Olympus UPlanApo 60 \times 1.2 NA water immersion objective was used to image the embryos on a JAI-40 CCD camera and locate the focal spot of the two-photon excitation. Illumination (200 fs, 76 kHz, 750 nm) was provided by a mode-locked Ti-Sapphire laser (Mira, Coherent). The incident power at the sample (≤ 4.5 mW) was measured with a Lasermate powermeter (Coherent). The fluorescence photons were collected through filters (AHF Analysentechnik, emission filter: 480/60 nm, excitation wavelengths: 750 nm for the experiments with **cF** and 720 nm with **cRA**) and optical fibers (FG200LCR multimode fiber, Thorlabs) and detected with avalanche photodiodes (SPCM-AQR-14, Perkin Elmer) coupled to an ALV-6000 correlator (ALV GmbH). The emission filters were chosen to match the emission characteristics of **RA** when bound to CRABP and CRBP.[7, 8] The intensity of the collected fluorescence emission and its temporal correlation function were recorded. The geometrical characteristics of the focal point were determined by Fluorescence Correlation Spectroscopy (FCS) measurements [9] on a fluorescein solution of known concentration (50 nM in 0.1 M NaOH). All the series of experiments reported in the present work have been performed in a regime of laser powers in which the examined fluorophores exhibit a quadratic dependence of the intensity of fluorescence emission on the illumination power.

²Embryo medium is composed of 0.80 g NaCl, 0.04 g KCl, 3.58 mg Na₂HPO₄, 6 mg KH₂PO₄, 0.144 g CaCl₂, 0.246 g MgSO₄·7H₂O, 0.35 g NaHCO₃ per liter of dd H₂O balanced with 1 M NaOH to pH 7.2.

Zebrafish embryo conditioning

Embryos were manually dechorionated at 1-3 somite stage. They were subsequently incubated in embryo medium supplemented with 1 μM **cF** or 10 μM **cRA** for 90 min. We located the two-photon focal spot in the dorsal part of the retina and continuously monitored the fluorescence intensity. Experiments were conducted on 12 embryos in each case. As a control, the same experiment was done on non-treated embryos.

Evaluation of possible photoinduced damages with two-photon excitation

Two-photon excitation requires a high flux of photons which may induce physical processes that could damage the embryos.

Light absorption which leads to energy dissipation as heat could be detrimental to the cell. Two types of light absorption processes can be here considered: water and endogenous chromophores. Schönle and Hell [10] have computed the temperature increase due to absorption by water molecules: it is in the 0.1 K range at 100 mW excitation power at 850 nm for an illumination duration of 1 s. It is negligible, at the laser intensities used here (less than 5 mW at the sample). Endogenous chromophores are present in a much smaller concentration than water but they can exhibit large molar absorption coefficients with one-photon absorption in the near IR. We can estimate the temperature increase due to absorption of a chromophore present at 1 mM concentration with a molar absorption coefficient of $5000 \text{ M}^{-1}\text{cm}^{-1}$ (a value similar to the one of hemoglobin [11]). Taking profit of the calculation by Schönle and Hell, we estimate this increase to be at most $\sim 5 \text{ K}$ at 10 mW laser power. Such an increase is not detrimental to the cell and we may therefore neglect the temperature increase resulting from absorption phenomena.

Another source of photoinduced physical damage is the possibility to ionize the cellular medium due to the electric field [11]: a plasma is formed at the focal point. This phenomenon is widely used in laser surgery to perform tissue ablation. This plasma creates a cavitation bubble made of the evaporated compounds. This bubble may emit shock wave that may modify the membrane permeability with a direct effect on cellular viability without affecting the cellular morphology [11]. In our experimental conditions (surfacic laser power: $10^{16} \text{ W}\cdot\text{m}^{-2}$), the threshold for cavitation can be estimated to be at a laser power of $\sim 11 \text{ mW}$ (see Noack et al., [12], Vogel et al. [13] and Sacchi [14]). Indeed when we applied powers larger than 10 mW, we observed the formation of a cavitation bubble and a shock wave which did not affect tissue morphology. However up to 5 mW average power, we never observed the formation of any cavitation bubble even when the embryo was illuminated for as long as one hour, and it eventually developed normally.

Retina malformation photoinduced upon **cRA** uncaging

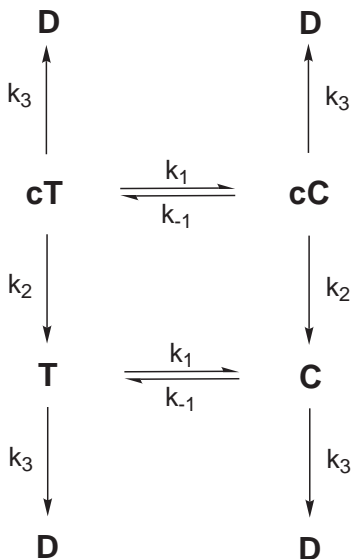
For retina malformation studies, we used a Nikon Diaphot inverted microscope modified for two-photon excitation (at non-detrimental incident power of 4.5 mW, see above) (to prevent unwanted uncaging of **cRA**, a 532 nm high pass filter was inserted in the brightfield illumination pathway). A Nikon CFI Plan Apochromat 20 \times (NA=0.75) air objective was used and its focal point geometry (waist diameter and focal point volume) characterized by FCS [9]. Imaging was done with a CCD camera (Hamamatsu ORCA C4742-95-12ER). Filters and dichroics mirrors were purchased from Omega Optical or Chroma Technology. The duration of the illumination was set by inserting an electro-mechanical shutter (SH05 beam shutter, Thorlabs) in the path of the laser beam.

Four different cells stacked in the z direction perpendicular to the plane of the retina were excited with the two-photon Ti:Sapphire laser source (750 nm, 4.5 mW incident power, durations 1 s) in manually dechorionated embryos previously incubated for 90 min in a 10 μ M **cRA** solution at the 4-14 somites stage. 23 embryos were illuminated and 14 exhibited unilateral malformations. This probability of malformation of $61 \pm 10\%$ is in excellent agreement with the 60% we could expect from the data of Hyatt et al. [15] and the illumination conditions used (the uncaging rate averaged over the cellular volume is 0.28 s^{-1} at 4.5 mW, 750 nm excitation).

The photoconversion kinetics of cRA upon UV illumination.

Kinetic model

In view of the photochemical behavior of all-*trans* retinoic acid,[16, 17] we considered three different processes to occur under UV illumination of a **cRA** solution: uncaging, photoisomerization and photodegradation. Scheme 2S displays the simple kinetic model which we adopted to analyze our data. The rate constants k_1 , k_{-1} relate to *trans/cis* photoisomerization, k_2 to uncaging, and k_3 to photodegradation. For a sake of simplicity, we here assume that i) the photoisomerization kinetics is similar for the caged ester and for the retinoic acid; ii) the uncaging rate as well as the photodegradation kinetics do not depend on the stereochemistry of the conjugation path.



Scheme 2S. Kinetic model that satisfactorily accounts for the photochemical events occurring during uncaging of the 4,5-dimethoxy-2-nitrobenzyl ester of all-*trans* retinoic acid **cRA**. **cT**, **cC**, **T**, **C**, **D** designate caged all-*trans* retinoic acid (**cRA**), caged *cis* retinoic acids, all-*trans* retinoic acid, *cis* retinoic acids and degradation products respectively.

Scheme 2S is associated to the system of differential equations Eqs.(1–4) linking the concentrations in **cT**, **cC**, **T**, **C**, and **D**:

$$\frac{dcT}{dt} = -(k_1 + k_2 + k_3)cT + k_{-1}cC \quad (1)$$

$$\frac{dcC}{dt} = k_1cT - (k_{-1} + k_2 + k_3)cC \quad (2)$$

$$\frac{dT}{dt} = k_2cT - (k_1 + k_3)T + k_{-1}C \quad (3)$$

$$\frac{dC}{dt} = k_2cC + k_1T - (k_{-1} + k_3)C \quad (4)$$

The four nontrivial eigenvalues of its determinant³ are $\lambda_1 = -(k_1 + k_{-1} + k_3)$, $\lambda_2 = -(k_2 + k_3)$, $\lambda_3 = -k_3$, and $\lambda_4 = -(k_1 + k_{-1} + k_2 + k_3)$. In principle, the photoactivation kinetics is characterized by four time scales: $\tau_i = -\frac{1}{\lambda_i}$. However if the photoisomerization kinetics is the fastest (as it indeed is; see Main Text and *vide infra*), the first and last time scales are similar $\tau_1 \approx \tau_4$. Under such conditions, only three characteristic times τ_1 , τ_2 and τ_3 associated to photoisomerization, uncaging and photodegradation should be observed for **cRA** under UV illumination. The temporal evolution of the concentrations in **cT**, **cC**, **T**, **C**, **D** should be correspondingly triexponential with τ_1 , τ_2 and τ_3 decay times: $A_1e^{-t/\tau_1} + A_2e^{-t/\tau_2} + A_3e^{-t/\tau_3}$. Much beyond τ_1 as in Figure 1c, this fitting law reduces to $A_2e^{-t/\tau_2} + A_3e^{-t/\tau_3}$.

Complementary experiments

Due to the large number of fitting parameters involved in the model displayed in Scheme 2S, we tried to evaluate separately the kinetics of the different pathways: photoisomerization, uncaging, and photodegradation, in the 365 nm UV illumination conditions used to test the **cRA** teratogenic effect on a whole zebrafish embryo. We used capillary electrophoresis and UV-Vis absorption to analyze the photoisomerization and photodegradation of all-*trans* retinoic acid and thus to derive orders of magnitude for k_1 and k_3 by relying on the similarities of the electronic demands in **cRA** and **RA**. To support the extracted k_2 value, we independently measured the uncaging rate constant of a substrate that did not photoisomerize nor photodegrade, since it was suggested that the uncaging kinetics did not markedly depend on the caged substrate, but on the photolabile moiety.[2]

Kinetics of photoisomerization and photodegradation of all-*trans* retinoic acid RA

Investigation by capillary electrophoresis In view of preceding work,[16, 17] we first used capillary electrophoresis (CE) to investigate the course of the photochemical reactions exhibited by all-*trans* retinoic acid **RA** under the UV illumination conditions used in our experiments on zebrafish embryos.

Three different peaks were observed in the CE electropherograms in the course of the UV illumination. They were attributed by comparison with reference samples of all-*trans*

3

$$\begin{vmatrix} \lambda + (k_1 + k_2 + k_3) & -k_{-1} & 0 & 0 \\ -k_1 & \lambda + (k_{-1} + k_2 + k_3) & 0 & 0 \\ -k_2 & 0 & \lambda + (k_1 + k_3) & -k_{-1} \\ 0 & -k_2 & -k_1 & \lambda + (k_{-1} + k_3) \end{vmatrix}$$

retinoic acid **RA** and two *cis* retinoic acids involved in its photoisomerization: the major 13-*cis* retinoic acid **C₁₃** and the minor 9-*cis* retinoic acid **C₉** (Chart 1S).

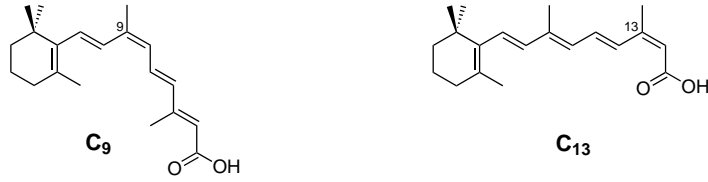


Chart 1S. Formula of the two *cis* retinoic acids identified from **RA** photoisomerization: 9-*cis* retinoic acid, **C₉**, and 13-*cis* retinoic acid, **C₁₃**.

As shown in Figure 1Sa, the relative concentration in **RA** drops as the relative concentrations of **C₁₃** and **C₉** increase.

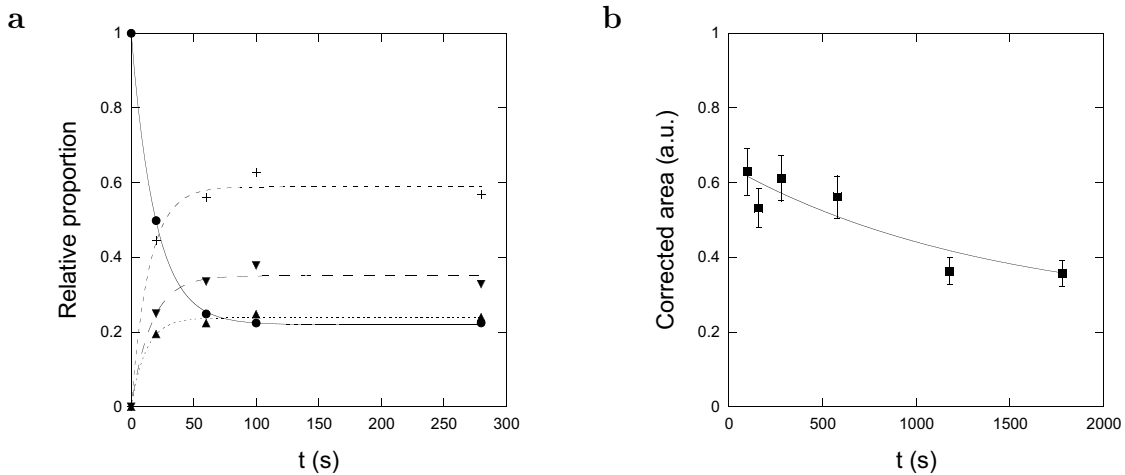


Figure 1S. One-photon irradiation of a 25 μM **RA** solution in acetonitrile/embryo medium 1/1 (v/v) at 293 K. **a:** Photoconversion extent as a function of time extracted from the CE electropherograms of the irradiated solution (circles: **RA**, uppointing triangles: **C₁₃**, downpointing triangles: **C₉**, crosses: **C = C₁₃ + C₉**; lines: exponential fits; **b:** Temporal evolution of the total amount **RA + C₁₃ + C₉** as extracted from CE electropherograms (squares: experimental points; solid line: exponential fit).

Clumping both *cis*-isomers into one species **C = C₁₃ + C₉**, one deduces on the short time scale where photoisomerization dominates:

$$\frac{T(t)}{T(0)} = \frac{k_{-1}}{k_1 + k_{-1}} + \frac{k_1}{k_1 + k_{-1}} e^{-(k_1 + k_{-1})t} \quad (5)$$

$$\frac{C(T)}{T(0)} = \frac{k_1}{k_1 + k_{-1}} - \frac{k_1}{k_1 + k_{-1}} e^{-(k_1 + k_{-1})t} \quad (6)$$

Both curves can be fitted with a single exponential curve to yield a similar estimate for $k_1 + k_{-1} = 6 \pm 0.5 \cdot 10^{-2} \text{ s}^{-1}$ providing $\tau_1 \approx 20 \text{ s}$ as an estimate of the relaxation time associated to photoisomerization.

The concentrations in the intermediates **RA**, **C₁₃**, and **C₉** subsequently remains stationary between 100 and 1000 s. In this intermediate kinetic regime, the retinoic acids

RA, **C**₁₃, and **C**₉ are submitted to a photoinduced dynamic exchange and the steady-state concentration in **RA** is equal to 20 % of the initial concentration of **cRA**.

On a longer time scale, one observes a continuous decrease of the total concentration of the various interconverting isomers of retinoic acid (**RA** + **C**₁₃ + **C**₉) (Figure 1Sb). An exponential fit to the data yields an estimate of the rate of retinoic acid degradation in our experimental conditions: $k_3 = 5 \pm 2 \cdot 10^{-4} \text{s}^{-1}$ (associated time scale $\tau_3 \approx 2000 \text{s}$).

Investigation by UV-Vis absorption Figure 2Sa displays the time evolution of the UV-Vis absorption of a **RA** solution that was irradiated under the UV illumination conditions used in our experiments on zebrafish embryos. As anticipated from the preceding CE investigation, the behavior is singular at the $\tau_1 \approx 20 \text{s}$ time scale: Up to 60 s, one observes wavelength shifts and absorption changes which are in line with the perturbation of the conjugation path associated to the photoisomerization process. The absorbance subsequently smoothly evolves as a function of time: The strong absorption band associated to the polyene motif drops whereas a much weaker absorption band in agreement with the less conjugated pattern expected for degradation products grows. The exponential fit of the absorbance associated to retinoic acids provides a value $k_3 = 6 \pm 2 \cdot 10^{-4} \text{s}^{-1}$ as an estimate of the rate of retinoic acid degradation rate which is in satisfactory agreement with the value derived from CE experiments (Figure 2Sb).

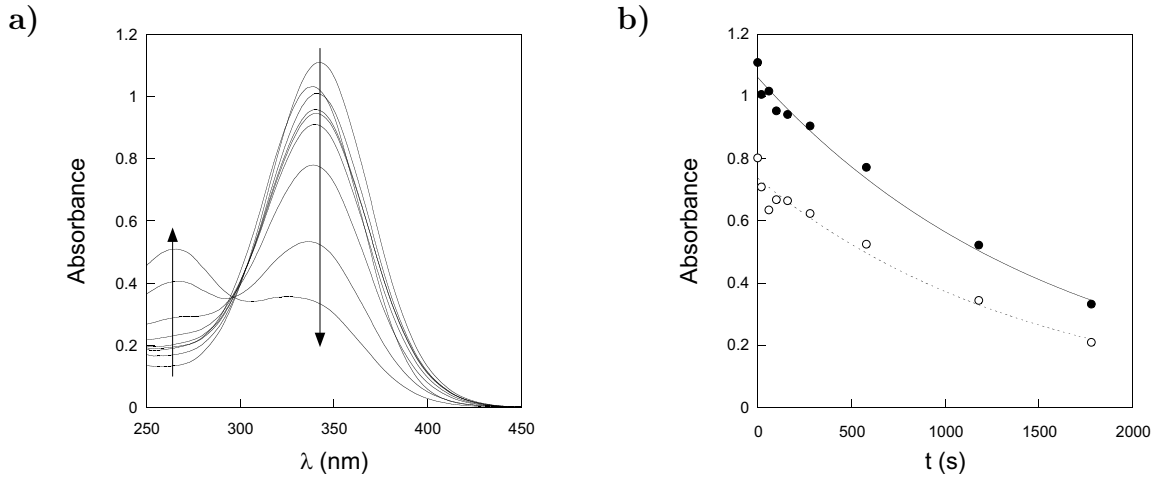
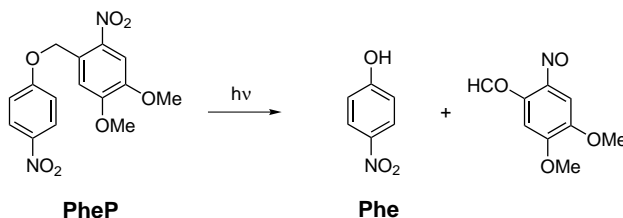


Figure 2S. One-photon irradiation of a 25 μM **RA** solution in acetonitrile/embryo medium 1/1 (v/v) at 293 K under the same illumination conditions as in Figures 1S. **a**: Evolution of the UV-Vis absorption spectra of the solution as a function of time ($t(\text{s})=0, 20, 60, 100, 160, 280, 580, 1180, 1780$); **b**: Evolution of the absorbance at 343 nm (disks) and at 364 nm (circles) as a function of time (markers: experimental points; lines: monoexponential fit).

Uncaging kinetics of a model compound upon UV illumination

To support the extracted value of the **cRA** uncaging rate k_2 , we examined the simpler 4,5-dimethoxy-2-nitrobenzyl caged substrate **PheP** which does not isomerize and yields upon UV illumination a strongly colored photoproduct that facilitates the study of its uncaging kinetics (Scheme 3S).[2]



Scheme 3S. Uncaging of **PheP** releases the weakly acidic substrate **Phe** that dissociates to yield a strongly absorbing anion.

Figure 3Sa displays the evolution of the absorbance of a 25 μM **PheP** solution as a function of time in the UV illumination conditions used in our experiments on zebrafish embryos. The **PheP** absorption band continuously drops whereas an absorption band near 400 nm corresponding to the released 4-nitrophenate anion increases with a typical rate: $k_2 = 3.5 \pm 0.5 \cdot 10^{-3} \text{ s}^{-1}$ associated to the time scale $\tau_2 \approx 300 \text{ s}$ (Figure 3Sb).

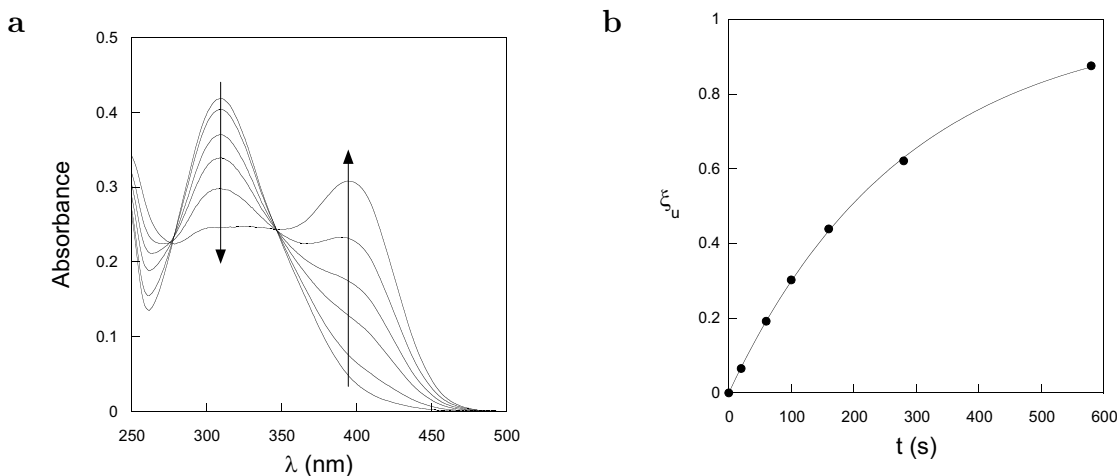


Figure 3S. One-photon irradiation of a 25 μM solution of **PheP** in acetonitrile/20 mM Tris pH=9 buffer 1/1 (v/v) at 293 K. **a:** Evolution of the UV-Vis absorption spectra of the solution as a function of time ($t(\text{s})=0, 20, 60, 100, 160, 280$); **b:** Uncaging extent ξ_u as a function of time as extracted from the evolution of the total absorbance at 400 nm, $A_{tot}(400, t)$: $\xi_u(t) = \frac{A_{tot}(400, t) - A_{tot}(400, 0)}{A_{tot}(400, \infty) - A_{tot}(400, 0)} = 1 - \exp(-k_2 t)$. Dots: experimental points; solid line: exponential fit.

Kinetics of **cRA** Uncaging/Photoisomerization/Photodegradation

The conclusion from the preceding complementary investigations is that the photoactivation kinetics of **cRA** should be characterized by three separate time scales: a fast

photoisomerization time: $\tau_1 \sim 20$ s followed by uncaging on a time scale $\tau_2 \sim 300$ s before photodegradation with characteristic time: $\tau_3 \sim 2000$ s.

The UV-Vis observations reported in the Main Text are in fair agreement with the preceding estimates. We derived: $\tau_1 \sim 20$ s, $\tau_2 \sim 400$ s, and $\tau_3 \sim 2000$ s. They are also in reasonable agreement with the capillary electrophoresis observation of $1 \pm 0.5 \mu\text{M}$ **RA** concentration after 280 s of illumination of $25 \mu\text{M}$ **cRA**.⁴ Indeed, at 280 s, we evaluate the uncaging extent to $\exp(-2.5 \cdot 10^{-3} \times 280) \approx 50$ %. In addition, **RA** would represent about 20 % of the photoreleased retinoic acids (*vide supra*). Thus one would expect to observe about $2.5 \mu\text{M}$ **RA**.

⁴**cRA** did not exit from the EC column under the required conditions to separate the retinoic acids; [4] **cRA** photoactivation kinetics was correspondingly derived from the observation on the intermediates **RA**, **C**₁₃, **C**₉ (the threshold for EC quantification was in the $1 \mu\text{M}$ range during the present series of EC).

Comparison of the phenotypes from trans and cis-retinoic acids

As uncaging is preceded by photoisomerizations (*vide supra*), we compared the significance of the concentration in the different identified retinoic acids on the phenotypes retained in that study.

We first investigated the teratogenicity of the retinoic acids. Embryos have been incubated at 128 cell stage in various concentrations of **RA**, **C₉**, and **C₁₃** for 90 min. Embryos were then washed and checked for malformations in the antero-posterior axis at 24 hpf. We observed that both cis retinoic acids produce phenotypes similar to the ones observed with comparable concentrations in all-trans retinoic acid.

We similarly performed control experiments related to retina malformation with **RA**, **C₉**, and **C₁₃**. 15 hpf embryos were incubated for 90 min in embryo medium supplemented with 1 μ M retinoic acid. Whereas **RA** yields a 38% malformation rate, the **C₉**-treated embryos yield a 19% malformation rate (17/88) and the **C₁₃**-ones a low 7% malformation rate (8/118) (they also generated developmental defects in the tail).

Teratogenic effects induced by UV illumination of **cRA** in injected embryos

In addition to the experiments reported in the Main Text, we also investigated the photoinduced teratogenic effects of **cRA** in injected embryos. Figure 4S displays the results.



Figure 4S. Dependence of the **cRA** photoinduced phenotype on the duration of UV illumination in zebrafish embryos after injection of 5 nl 0.1 mM **cRA** in 32 cell embryos and subsequent one photon 365 nm illumination for 40 (a), 160 (b) or 240 s (c); (d) control (injection of 5 nl 1% DMSO).

For the longest illumination durations, the zebrafish embryos develop normally which suggests that, at that stage of development (32 cell embryo), the various retinoids are efficiently photodegraded *in vivo*. This is in accordance with the *in vitro* experiments which show that **RA** photorelease upon **cRA** uncaging occurs only over a defined window of illumination duration.

The two-photon uncaging kinetics of **cRA** *in vivo*.

General kinetic model

Incubation of the embryo in a solution of caged compound **cA** (either the caged fluorophore **cF** or **cRA**) is assumed to lead to an initially uniform distribution of **cA** throughout the embryo (initial concentration cA_0). Introducing **A** and **G** as the active substrate and the caging group respectively, the uncaging reaction:



is considered to take place in the illuminated volume V_{exc} resulting from laser focusing with a rate k_{unc} which has been derived by Kiskin et al.: [18]

$$k_{unc} = 0.737\delta_u \frac{T}{\tau_P} \left(\frac{\lambda}{\pi h c \omega_{xy}^2} \right)^2 P^2 \quad (8)$$

$\delta_u = 22$ mGM (1 GM = 10^{-50} cm⁴.s/photon) is the uncaging cross section of the 4,5-dimethoxy-2-nitrobenzyl caging group for two-photon absorption at the excitation wavelength $\lambda = 750$ nm, [2] $T = 13.6$ ns is the period of the laser pulses of incident power P , duration $\tau_P = 200$ fs and waist at the focal point ω_{xy} ($0.3 \mu\text{m}$ for a $60\times$ objective of NA=1.2; measured by Fluorescence Correlation Spectroscopy with two-photon excitation).

Neglecting diffusion of the reactant and products of the reaction (7) in and out of the cells within the uncaging timescales, each embryo cell can be assumed as a closed system, of volume V . Noticing that the effective uncaging time $\tau_2 = 1/k_2 = V/(k_{unc}V_{exc}) \sim 1$ s is larger than the diffusion time in the volume V of the cell ($\tau_V \simeq 20$ ms), the reactant and products can be considered to be homogeneously distributed within the cell. Then the concentrations in **cA** and **A** obey:

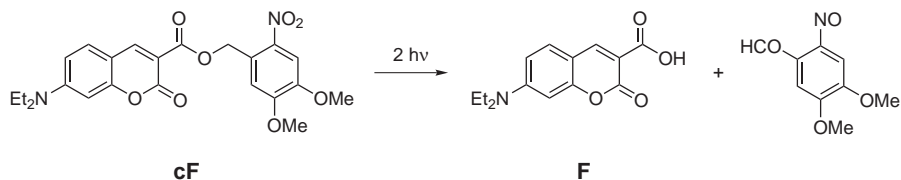
$$\frac{dcA}{dt} = -\frac{dA}{dt} = -k_2cA \quad (9)$$

which solution is:

$$A(t) = cA_0 (1 - e^{-k_2t}) \quad (10)$$

Preliminary experiments with a caged fluorophore **cF**

We designed a favorable caged model fluorophore for **cRA**: **cF** [2] is a non-fluorescent caged molecule sharing with **cRA** its photolabile protecting group and a similar hydrophobicity/hydrophilicity balance (Scheme 4S). In contrast to **cRA**, it releases a strongly fluorescent coumarin **F** upon uncaging which makes it the most appropriate for i) evaluating the preceding kinetic model; ii) measuring the uncaging rate at a given laser power; iii) characterizing the targeted retina cells.



Scheme 4S. Uncaging of the model caged compound **cF** releasing the strongly fluorescent coumarin **F** upon two-photon excitation.

Figure 5Sb displays the increase in fluorescence intensity $\delta I(t)$ arising from the photorelease of the fluorescent substrate **F** in a single cell of the developing retina of a zebrafish embryo, previously incubated in a **cF** solution. Figure 5Sb also shows that the intensity exhibits an exponential growth as predicted by the expression (Eq.10) derived from the kinetic model.

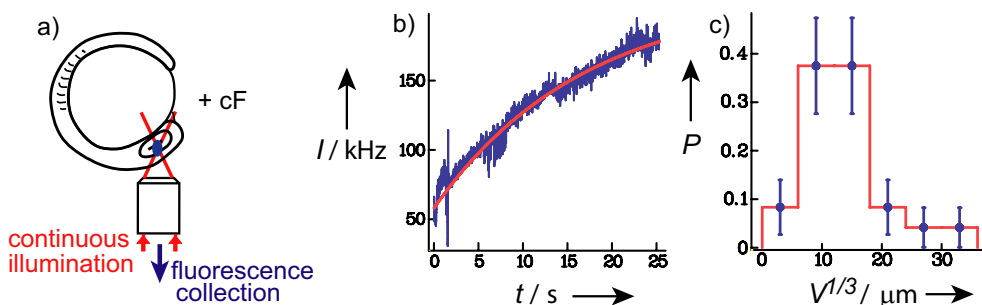


Figure 5S. Two photon **cF** uncaging *in vivo*. **a**: Principle of the experiment. **b**: Increase in fluorescence observed upon illuminating at 1.8 mW laser power a single retina cell of a manually dechorionated 4-14 somite embryo previously incubated for 90 min in 1 μM **cF**. The rise of the fluorescence intensity $I(t)$ results from uncaging the fluorescent coumarin **F** from its non-fluorescent precursor **cF**. Continuous line: fit to $I(t) = I_{max}(1 - e^{-k_2 t})$ with rate constant $k_2 = 0.04\text{ s}^{-1}$; **c**: Probability distribution of cell sizes deduced from the distribution of the values of k_2 measured in different cells as in **b**. Error bars represent s.e.m.

Due to variation in cellular volume, the extracted values of k_2 vary from cell to cell. The average value deduced from fits with Eq.(10) from data obtained in different cells yields $\langle \tau_2 \rangle = 25\text{ s}^{-1}$ at an excitation power of 1.8 mW. We measured V_{exc} by Fluorescence Correlation Spectroscopy with two-photon excitation of a fluorescein solution of known concentration and calculated k_{unc} from Eq. 8 to extract the volume V of the illuminated cell from the relaxation time τ_2 . Figure 5Sc shows the resulting distribution of cell size typically evaluated as $V^{1/3}$. The mean value $\langle V^{1/3} \rangle = 13.5 \pm 6\ \mu\text{m}$ (error is standard deviation) agrees with accepted values for the size of the targeted cells.

Altogether, this series of experiments:

- shows that two-photon **cF** uncaging obeys Eq. (10) and leads to the release of the **F** substrate in a single cell that can be considered as impermeable on the timescale

of the experiment (a few minutes⁵);

- calibrates the uncaging rate of the 4,5-dimethoxy-2-nitrobenzyl caging moiety. We found $\langle k_2 \rangle = 0.04 \text{ s}^{-1}$ at an excitation power of 1.8 mW and we checked that k_2 was quadratically depending on the laser power P (thus one should expect $\langle k_2 \rangle = 0.012 \text{ s}^{-1}$ at an excitation power of 1 mW; see Main Text);
- provides the typical size distribution of the targeted retina cells.

⁵The structurally close but more hydrophobic retinol has been reported to diffuse out of cells with a 2.5 min timescale [19]. We thus expect the timescale for **RA** diffusion to be much larger, this being consistent with the absence of diffusion of **RA** out of the illuminated cell over several minutes.

References

- [1] V. R. Shembekar, Y. Chen, B. K. Carpenter, G. P. Hess, *Biochemistry* **2005**, *44*, 7107–7114.
- [2] I. Aujard, C. Benbrahim, M. Gouget, O. Ruel, J.-B. Baudin, P. Neveu, L. Jullien, *Chem. Eur. J.* **2006**, *12*, 6865–6879.
- [3] A recent report also underlines the innocuousness of 365 nm UV light in the zebrafish system. See I. A. Shestopalov, S. Sinha, J. K. Chen, *Nat. Chem. Biol.* **2007** *3*, 650–651.
- [4] D. K. Bempong, I. L. Honigberg, N. M. Meltzer, *J. Pharm. Biomed. Anal.* **1993**, *11*, 829–833.
- [5] *The Zebrafish Book; A guide for the laboratory use of zebrafish (Danio rerio)*, M. Westerfield, University of Oregon Press, Eugene, **2000**.
- [6] N. Gagey, P. Neveu, L. Jullien, *Angew. Chem. Int. Ed. Engl.* **2007**, *46*, 2467–2469.
- [7] J. S. Bailey, C. H. Siu, *J. Biol. Chem.* **1988**, *263*, 9326–9332.
- [8] P. N. MacDonald, D. E. Ong, *J. Biol. Chem.* **1987**, *262*, 10550–10556.
- [9] O. Krichevsky, G. Bonnet, *Rep. Prog. Phys.* **2002**, *65*, 251–297.
- [10] A. Schönle, S. W. Hell, *Opt. Lett.* **1998**, *23*, 325–327.
- [11] A. Vogel, V. Venugopalan, *Chem. Rev.* **2003**, *103*, 577–644.
- [12] J. Noack, D. X. Hammer, G. D. Noojin, B. A. Rockwell, A. Vogel, *J. App. Phys.* **1998** *83*, 7488–7495.
- [13] A. Vogel, J. Noack, G. Hüttman, G. Paltauf, *App. Phys. B* **2005**, *85*, 1015–1047.
- [14] C. A. Sacchi, *J. Opt. Soc. Am. B* **1991**, *8*, 337–345.
- [15] G. A. Hyatt, E. A. Schmitt, N. Marsh-Armstrong, P. McCaffery, U. C. Drager, J. E. Dowling, *Development* **1996**, *122*, 195–204.
- [16] R. W. Curley Jr, J. W. Fowble, *Photochem. Photobiol.* **1988**, *47*, 831–835.
- [17] A. Murayama, T. Suzuki, M. Matsui, *J. Nutr. Sci. Vitaminol.* **1997**, *43*, 167–176.

- [18] N. Kiskin, R. Chillingworth, J. A. McCray, D. Piston, D. Ogden, *Eur. Biophys. J.* **2002**, *30*, 588–604.
- [19] C. C. Chen, J. Heller, *J. Biol. Chem.* **1977**, *252*, 5216–5221.